Electronic Supplementary Material (ESI) for ChemComm.

Zirconium bistriazolylpyridine phosphonate materials for efficient, selective An(III)/Ln(III) separations

Jessica Veliscek-Carolan, Aditya Rawal

Table of Contents

Synthesis

Organic Precursor Synthesis

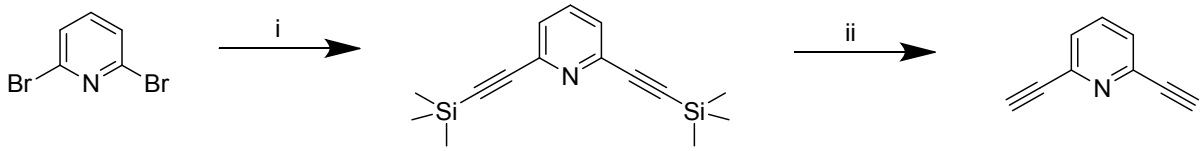

Scheme S1: Synthesis of 2,6-diethynylpyridine described by Yuan et al[1]. Conditions: (i) TMS-acetylene, $Pd(PPh_3)_4$, CuI, THF/diisopropylamine, 50 °C, 6 h, yield 90 %; (ii) K_2CO_3, methanol/diethyl ether, yield 36 %.

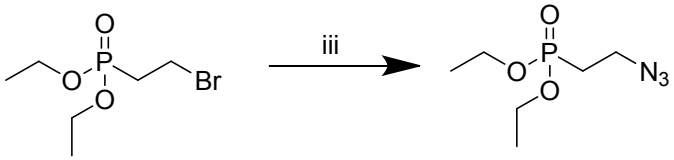

Scheme S2: Synthesis of diethyl-2-azidoethylphosphonate described by Ma et al[2]. Conditions: (iii) NaN_3, acetone, reflux 24 h, yield 72 %.

Synthesis of 2,6-bis(1,2,3-triazol-1-ethanephosphonate)pyridine ("PTP")

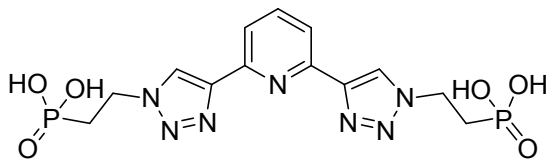

2,6-bis(1,2,3-triazol-1-ethanephosphonate)pyridine was prepared according to the literature,[3-4] with modifications. 2,6-diethynylpyridine (0.39 g, 3.06 mmol) and 2-azidoethylphosphonic acid (1.82 g, 8.76 mmol, 2.9 equiv.) were dissolved in a 1:1 mixture of isopropanol and water (22 mL). Sodium ascorbate (0.12 g, 0.62 mmol, 0.2 equiv) and $CuSO_4.5H_2O$ (16 mg, 0.06 mmol, 0.02 equiv.) were then added. The resulting light brown, opaque solution was stirred at room temperature for 44 h. The isopropanol was removed under vacuum and the remaining aqueous solution was extracted with CH_2Cl_2 (3 x 20 mL). The combined organic layers were dried over Na_2SO_4 and the solvent removed under vacuum. The resulting crude product was purified via column chromatography (95:5 CH_2Cl_2:methanol) to afford 2,6-bis(1,2,3-triazol-1-diethylethanephosphonate)pyridine as a brown oil (0.91 g, 1.72 mmol, 56 % yield). ^{1}H NMR ($CDCl_3$, 400 MHz): δ (ppm) 1.31 (t, *J* = 6.8 Hz, 12H), 2.49 (m, 4H), 4.11 (m, 8H), 4.72 (m, 4H), 7.86 (t, *J* = 7.8 Hz, 1H), 8.08 (d, *J* = 7.8 Hz, 2H), 8.27 (s, 2H).

Hydrolysis of 2,6-bis(1,2,3-triazol-1-diethylethanephosphonate)pyridine (0.91 g, 1.72 mmol) was achieved by addition of concentrated HCl (37 %, 15 mL) and reflux at 80 °C with stirring for 48 h. The solvent was removed under vacuum to afford 2,6-bis(1,2,3-triazol-1-

ethanephosphonate)pyridine as a brown oil (0.65 g, 1.52 mmol, 90 % yield). ^{1}H NMR (DMSO-d_6, 400 MHz): δ (ppm) 2.26 (m, 4H), 4.59 (m, 4H) 7.94 (m, 3H), 8.69 (s, 2H); ^{31}P NMR (DMSO-d_6, 400 MHz): δ (ppm) 21.1.

ZrPTP synthesis

All reactants were purchased from Sigma Aldrich and were reagent grade or higher. Reagents were used as supplied without further purification.

2,6-bis(1,2,3-triazol-1-ethanephosphonate)pyridine (214 mg, 0.5 mmol) was mixed with 25 mL MilliQ water (for ZrPTP_a1) or dimethylformamide (for ZrPTP_o1) and zirconium(IV) chloride (117 mg, 0.5 mmol). The resulting suspension was stirred at room temperature for 1 h in a plastic beaker. The suspension differed in appearance depending on the solvent used. In aqueous solution it appeared as pale brown and opaque and settled quickly when stirring was stopped. In dimethylformamide it appeared pale brown but more transparent and gel-like, without settling. The suspension was then transferred to a parr reactor vessel for hydrothermal treatment at 120 ^{o}C for 24 h. After cooling, the products were vacuum filtered through qualitative filter paper, washed with MilliQ water and air dried. The resulting light brown solid was ground to a fine powder in a mortar and pestle.

ZrPTP_a2, _a3 and _o2 were synthesised in the same manner but using less equivalents of 2,6-bis(1,2,3-triazol-1-ethanephosphonate)pyridine.

Characterisation

X-ray diffraction (XRD) data were obtained on a Panalytical Empyrean diffractometer using Cu Kα radiation and a PIXcel 3D detector. Nitrogen adsorption-desorption isotherms for dried powders were obtained by multipoint nitrogen gas sorption experiments at 77 K after degassing at 150 ^{o}C on a Micromeritics ASAP 2420 porosimeter. Surface areas were estimated according to the Brunauer-Emmett-Teller (BET) method while pore volume and pore size distributions were calculated using the Barrett-Joyner-Halenda (BJH) method based on the desorption branch. Scanning electron microscopy (SEM) was performed on a Zeiss Ultra Plus electron microscope operating at 10-15 kV. For elemental analysis, samples were digested in conc. H_2SO_4 for a minimum of 48 h and the resulting solutions were diluted before ICP-MS analysis to determine the Zr and P contents. Inductively coupled plasma – mass spectrometry (ICP-MS) for elemental analysis of solutions before and after sorption experiments was performed on a Varian 820-MS instrument. Samples for ICP-MS analysis were diluted 1:10 in 3 % HNO3 and concentrations were measured against internal standards. Gamma counting was performed on a Hidex AMG - Automatic Gamma Counter. Fourier Transform Infra-Red (FTIR) spectra were obtained on a Nicolet Nexus 8700 FTIR Spectrometer (Thermo Electron Corporation) using the Smart iTR attenuated total reflectance (ATR) accessory. Solid-state NMR spectra were recorded on a Bruker Biospin Avance III solid state 300 MHz instrument and a Bruker Avance III solid state 700 MHz NMR spectrometer using a Bruker 4 mm double resonance magic-angle spinning (MAS) probehead with a MAS

frequency of 12 kHz. Spectral deconvolution of one-dimensional NMR spectra was performed using the DMFIT program with half-gaussian half-lorentzian peak shapes.[5]

Sorption methodology

To prepare 10 ppb ^{241}Am solutions, 28 µL aliquots of a ^{241}Am stock solution (2.1 MBq/mL, 3 M nitric acid, specific activity ^{241}Am = 118.4 MBq/mg) were diluted to 50 mL with either 0.1 M (pH 1) or 0.01 M (pH 2) nitric acid. To prepare the 10 ppb Eu solutions, a 3.6 mL spike of ^{152}Eu stock solution (1.0 kBq/mL, specific activity ^{152}Eu = 6.7 GBq/mg) and 20 µL of 10 ppm carrier Eu were diluted to 20 mL with 0.01 - 0.1 M nitric acid. To prepare mixed ^{241}Am and Eu solution containing 10 ppb of each element (1:1 Am:Eu), 11.2 µL aliquot of the ^{241}Am stock solution and 20 µL of 10 ppm carrier Eu were diluted to 20 mL with 0.01 M nitric acid. Mixed ^{241}Am and Eu solution containing 10 ppb ^{241}Am and 400 ppb Eu (1:40 Am:Eu) was similarly prepared but using 80 µL of 100 ppm carrier Eu.

Individual element sorption experiments were performed with pH 1-2 10 ppb ^{241}Am or spiked ^{152}Eu solutions while competitive sorption experiments were performed with pH 2 mixed ^{241}Am/Eu solutions. All sorption experiments were performed in duplicate via the batch contact method and using a constant volume-to-mass ratio of 200 mL/g. The solutions and powders were contacted in plastic screw-cap vials. Samples were shaken on a vertical mixer at a constant speed of approximately 10 rpm for a period of 24 h (or for designated time). After sorption, the suspensions were filtered through individual 0.45 µm syringe filters.

The resulting liquids from individual element sorption experiments were analysed by gamma counting two 0.5 mL aliquots of the solutions before sorption and a 0.5 mL aliquot from each duplicate sample after sorption, for 10 min. For ^{241}Am, a counting window of 40-80 keV was used and for ^{152}Eu a counting window of 100-1400 keV was used. For the competitive sorption experiments, analysis was undertaken via gamma counter for ^{241}Am (40-80 keV, 10 min) and ICP-MS for Eu. However, the concentration of Eu after sorption from the 1:1 Am:Eu was too low to be analysed by ICP-MS. Therefore, the 1:1 Am:Eu solution was spiked with ^{152}Eu and the resulting solution after sorption was analysed via gamma counting (150-1400 keV, 1 h). Hence, for the 1:1 Am:Eu competitive sorption experiment, the reported ^{241}Am K_d was calculated using data from the sorption experiment with inactive Eu (to prevent interference of from ^{152}Eu in the counting region of 40-80 keV) but the reported Eu K_d was calculated using data from the sorption experiment with ^{152}Eu spike.

Errors in the reported partition coefficient values were calculated from the standard deviation of the gamma counting results. If the standard deviation was less than 1 % of the measured cpm value, an error of 1 % was applied.

X-Ray Diffraction (XRD)

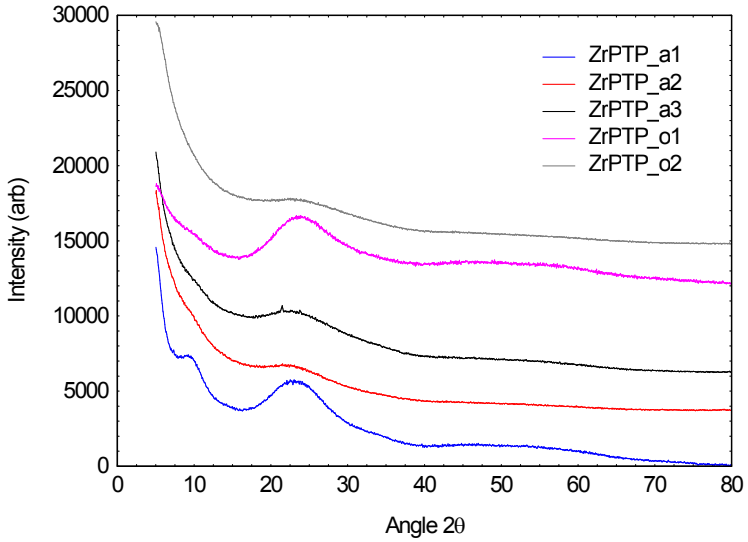

Figure S1: XRD patterns of ZrPTP materials.

Figure S1 shows that ZrPTP_a1 and ZrPTP_o1, both of which had a molar ratio P/Zr of 2.0, had more prominent peaks in their XRD spectra than the ZrPTP materials with lower molar P/Zr ratios. The broad peaks in the XRD spectra of ZrPTP_a1 and ZrPTP_o1 indicate a disordered layered structure with a d-spacing of approx. 9 Å. When the molar ratio P/Zr was decreased, this layered structure no longer appeared to form and instead more disordered materials were produced. This is likely because a ligand:Zr ratio of 1:1 (and hence molar P/Zr of 2.0) was required to produce the layered structure.

Elemental Analysis

Table S1: Elemental analysis of ZrPTP materials

Sample	***ICP-MS***		***Molar P/Zr***
	%Zr	**%P**	
ZrPTP_a1	11.1 ± 0.3	7.5 ± 0.1	2.0 ± 0.1
ZrPTP_a2	13.9 ± 0.4	7.8 ± 0.1	1.6 ± 0.1
ZrPTP_a3	16.6 ± 0.6	7.5 ± 0.3	1.3 ± 0.1
ZrPTP_o1	9.2 ± 0.3	6.3 ± 0.3	2.0 ± 0.2
ZrPTP_o2*	19.4 ± 0.1	4.7 ± 0.2	0.7 ± 0.03

*Zrbtp_o2 didn't appear to fully dissolve in conc. H_2SO_4, some small particles were still visible after shaking for 1 week.

ZrPTP_a1 has P and Zr content consistent with $ZrC_{13}H_{17}N_7O_6P_2$.**$16H_2O$** (P/Zr 2.0, MM 808.9).
ZrPTP_a2 has P and Zr content consistent with $Zr_{1.2}C_{13}H_{17}N_7O_6P_2$.**$14H_2O$** (P/Zr 1.7, MM 791.1).
ZrPTP_a3 has P and Zr content consistent with $Zr_{1.5}C_{13}H_{17}N_7O_6P_2$.**$14H_2O$** (P/Zr 1.3, MM 818.5).
ZrPTP_o1 has P and Zr content consistent with $ZrC_{13}H_{17}N_7O_6P_2$.**$27H_2O$** (P/Zr 2.0, MM 1007).
ZrPTP_o2 has P and Zr content consistent with $Zr_{2.8}C_{13}H_{17}N_7O_6P_2$.**$35H_2O$** (P/Zr 0.7, MM1314.8).

Nitrogen Porosimetry

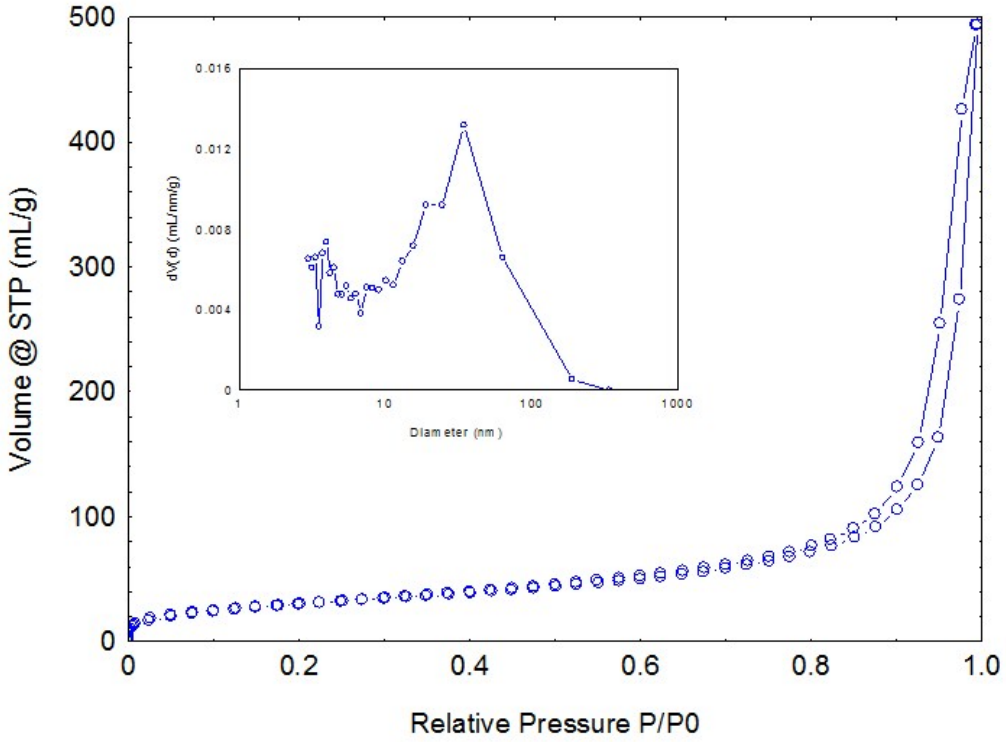

Figure S2: Nitrogen sorption isotherm and pore size distribution (inset) for ZrPTP_a1

The nitrogen sorption isotherm for ZrPTP_a1 was type II/IV suggesting the presence of macropores and mesopores. The BET surface area of ZrPTP_a1 was 109 m^2/g with 5 m^2/g due to micropores. The BJH desorption pore volume of ZrPTP_a1 was 0.75 mL/g and the pore diameter was 10-80 nm (mesopores and macropores). Nitrogen porosimetry on ZrPTP_o1 indicated the surface area of this sample was below the instrument limit.

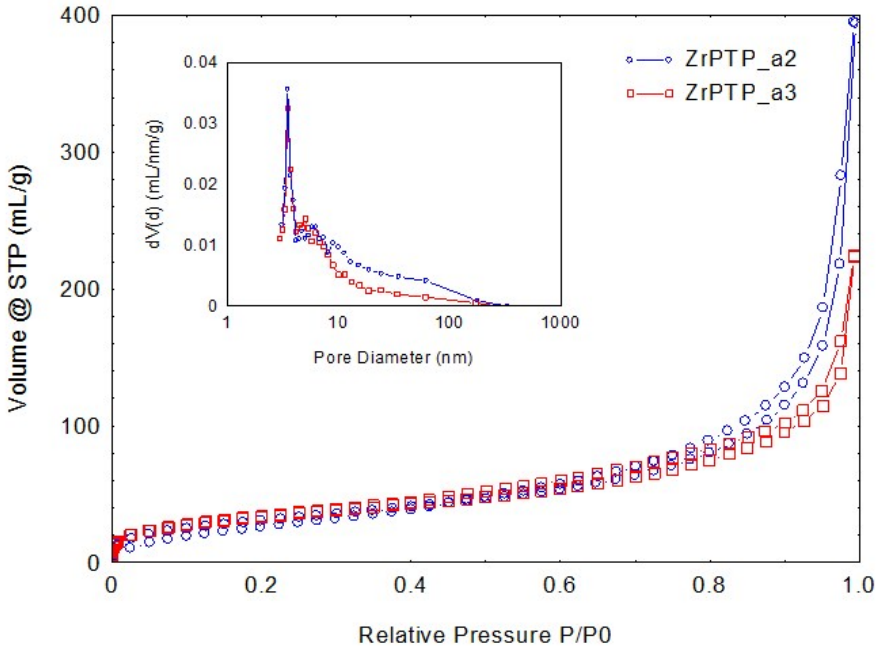

Figure S3: Nitrogen sorption isotherms and pore size distribution (inset) for ZrPTP_a2 and ZrPTP_a3

As for ZrPTP_a1, the nitrogen sorption isotherms for ZrPTP_a2 and ZrPTP_a3 were type II/IV suggesting the presence of macropores and mesopores. The BET surface areas of ZrPTP_a2 and ZrPTP_a3 were 113 and 122 m^2/g, respectively. Hence the surface areas of all three of the ZrPTP_a materials were similar.

The BJH desorption pore volume of ZrPTP_a2 and ZrPTP_a3 were 0.61 and 0.32 mL/g, respectively. Hence, pore volume decreased with the molar ratio P/Zr for the ZrPTP_a series. This was consistent with the pore size data, which indicated both ZrPTP_a2 and ZrPTP_a3 had predominantly smaller 3-4 nm pores as opposed to the 10-80 nm pores in ZrPTP_a1.

Scanning Electron Microscopy (SEM)

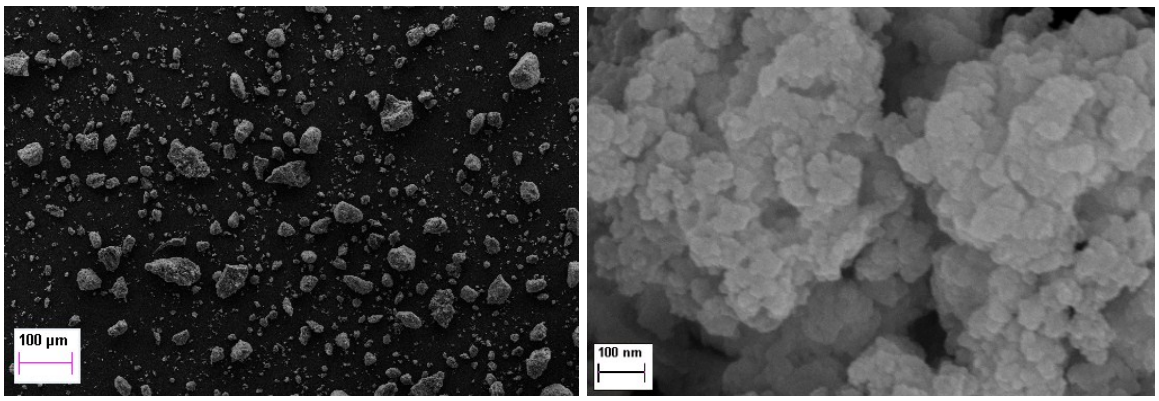

Figure S4: SEM images of ZrPTP_a2

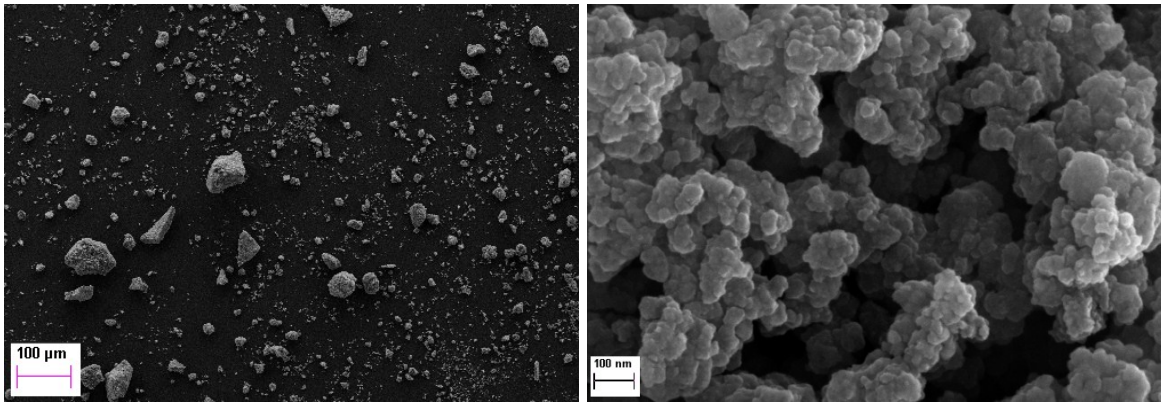

Figure S5: SEM images of ZrPTP_a3

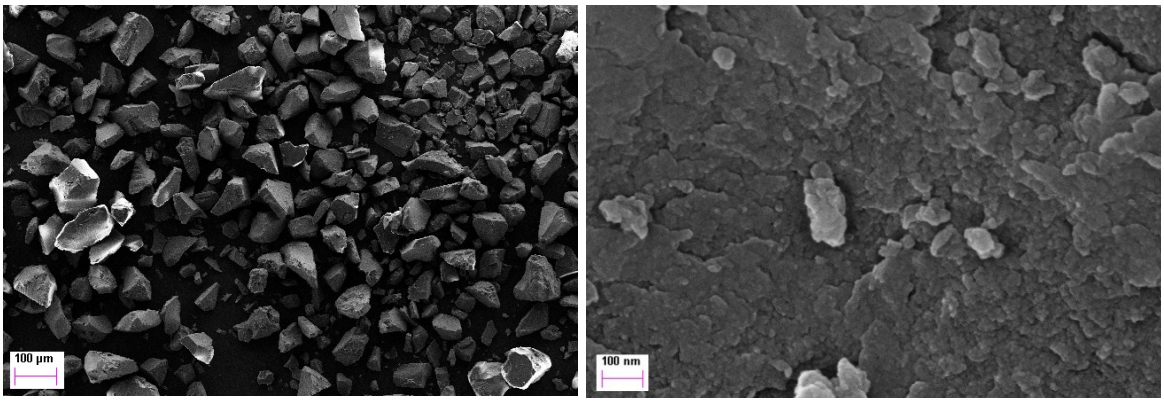

Figure S6: SEM images of ZrPTP_o2

Fourier Transform Infrared Spectroscopy (FTIR-ATR)

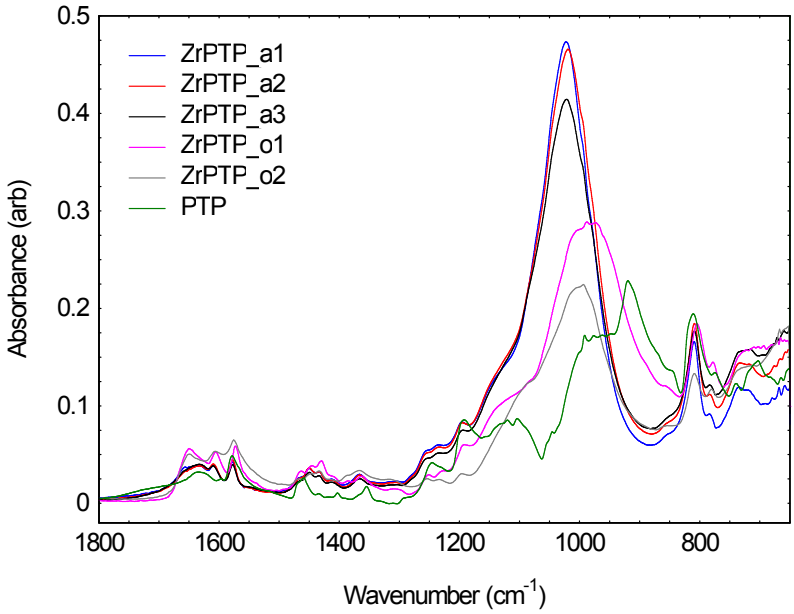

Figure S7: FTIR-ATR spectra of ZrPTP materials.

The data in Figure S5 shows that for the ZrPTP_a series, decreasing the molar ratio P/Zr did not substantially change the position of the P-O absorbance band. However, for the ZrPTP_o series, decreasing the molar ratio P/Zr caused the P-O absorbance band to shift further towards higher wavenumber, indicating that there were fewer P-OH groups and more metal coordinated P-OZr groups in ZrPTP_o2 than in ZrPTP_o1. This change was likely observed in the ZrPTP_o series but not the ZrPTP_a series because the change in molar ratio P/Zr between ZrPTP_o1 and _o2 was substantially larger than that between ZrPTP_a1 and _a3 (see Table S1).

Nuclear Magnetic Resonance Spectroscopy (NMR)

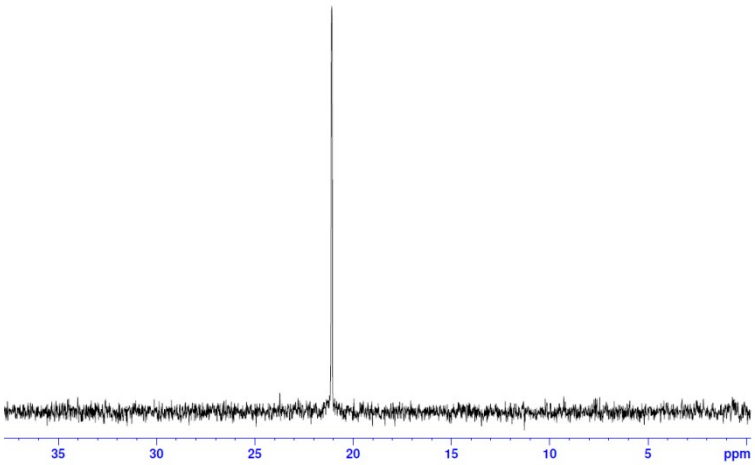

Figure S8: ^{31}P NMR of PTP ligand

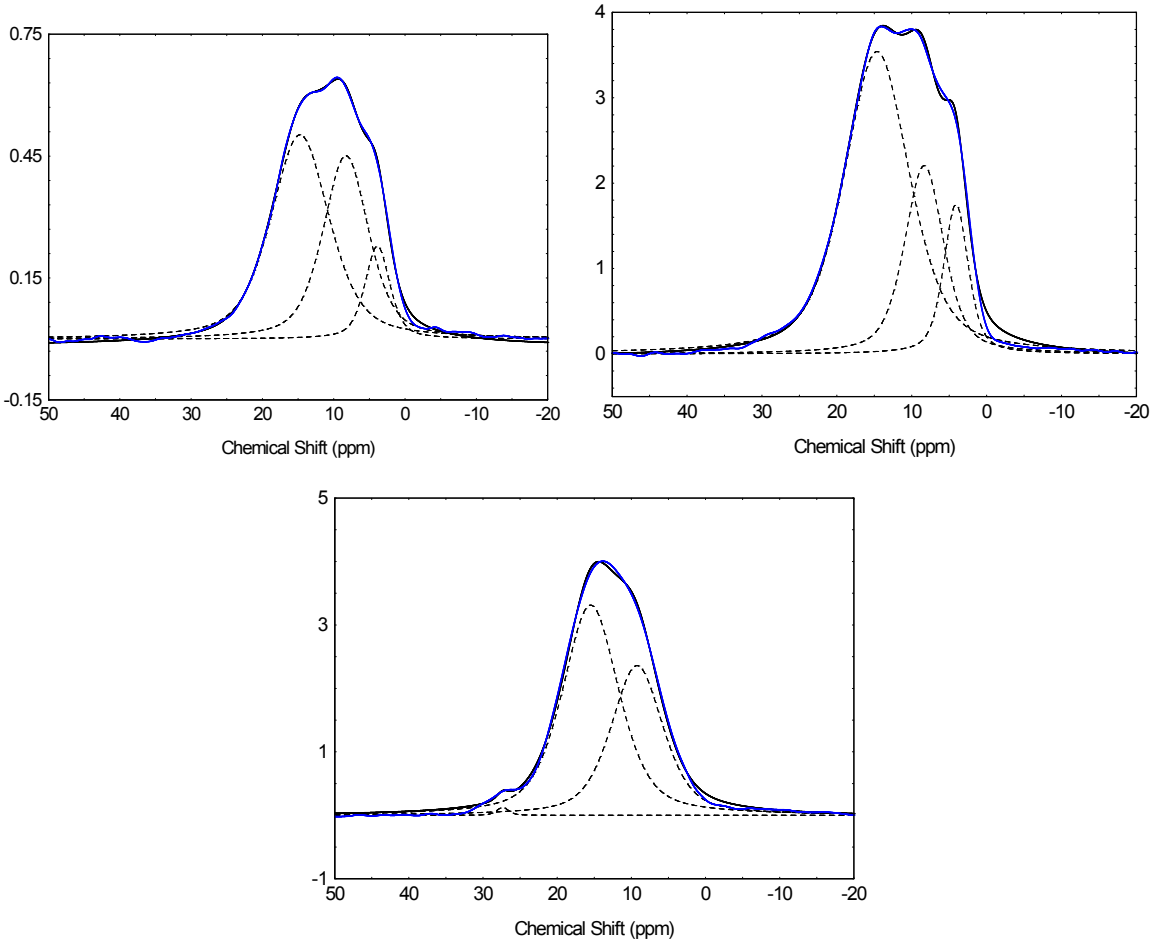

Figure S9: ^{31}P MAS NMR spectra of ZrPTP_a2 (top left), ZrPTP_a3 (top right) and ZrPTP_o2 (bottom).

Table S2: Relative intensities of peaks in ^{31}P MAS-NMR spectra of ZrPTP materials

Chemical shift (ppm)	**4 to 5 $P(O)(OZr)_2$**	**8 to 9 P(O)(OH)(OZr)**	**15 to 16 P(O)(OZrO)**	**27 $P(O)(OZr)(OZr_2)$[6]**
ZrPTP_a1	0.16	0.47	0.37	
ZrPTP_a2	0.14	0.32	0.54	
ZrPTP_a3	0.12	0.29	0.59	
ZrPTP_o1	0.09	0.62	0.29	
ZrPTP_o2		0.39	0.60	0.01

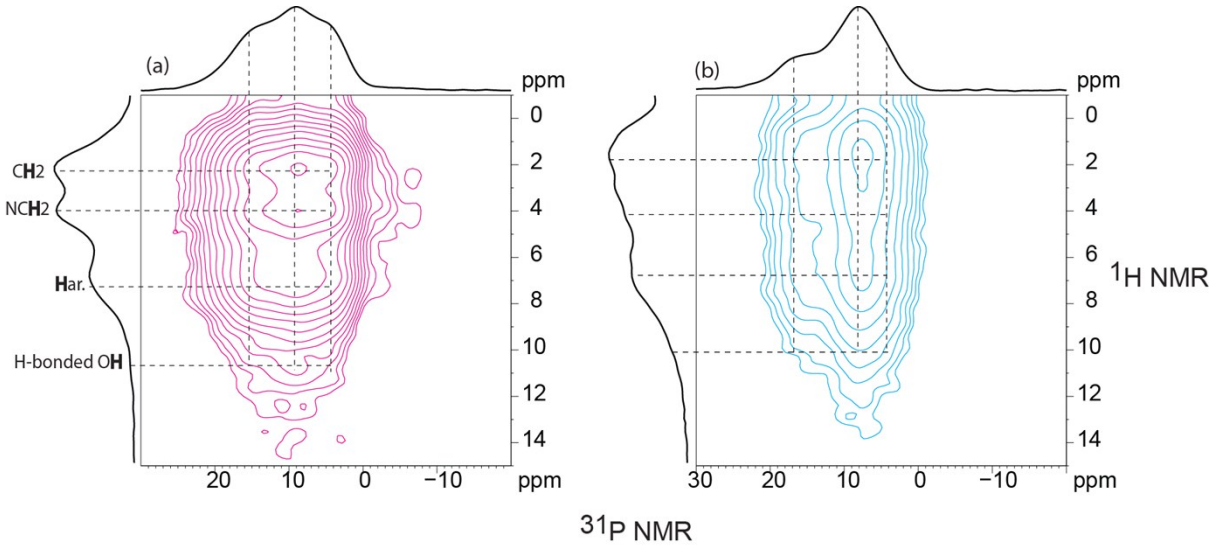

Figure S10: 2D ^{1}H-^{31}P HetCor NMR of ZrPTP_a1 (left) and ZrPTP_o1 (right).

The ^{1}H signals at approximately 2, 4 and 7 ppm in Figure S8 were assigned as C**H$_2$**-PO_3H_2, N-C**H$_2$** and aromatic C**H** environments of the btp ligand. The substantially weaker ^{1}H signal at approximately 10 ppm is likely due to tightly H-bonded water.

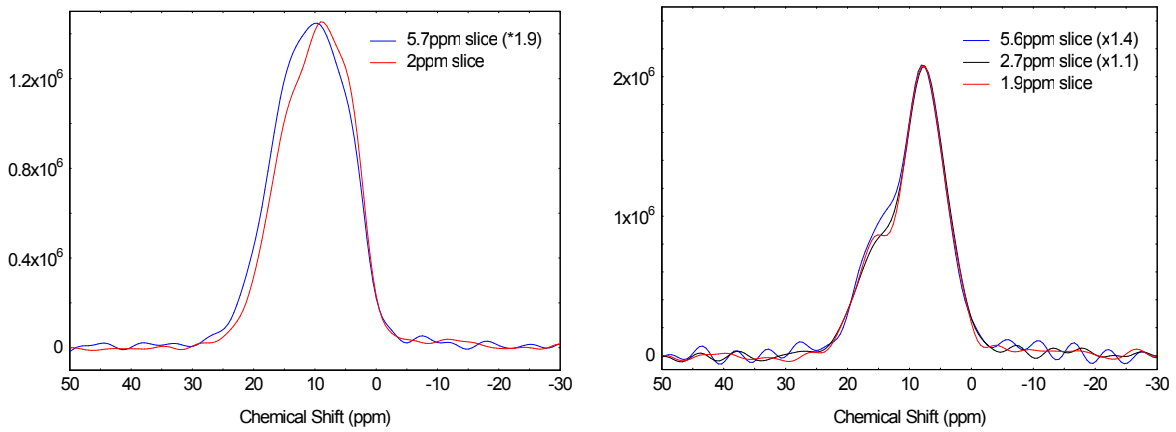

Figure S11: ^{31}P MAS NMR spectra of Zrbtp_a1 (left) and Zrbtp_o1 (right) at different ^{1}H environments, from the 2D NMR spectra.

References

1 J. Yuan, X. Fang, L. Zhang, G. Hong, Y. Lin, Q. Zheng, Y. Xu, Y. Ruan, W. Weng, H. Xia and G. Chen, *J Mater Chem*, 2012, **22**, 11515.

2 C. Ma, T. Bian, S. Yang, C. Liu, T. Zhang, J. Yang, Y. Li, J. Li, R. Yang and W. Tan, *Anal Chem*, 2014, **86**, 6508.

3 E. Brunet, O. Juanes, L. Jiménez and J. C. Rodríguez-Ubis, *Tetrahedron Lett*, 2009, **50**, 5361.

4 F. Himo, T. Lovell, R. Hilgraf, V. V. Rostovtsev, L. Noodleman, K. B. Sharpless and V. V. Fokin, *J. Am. Chem. Soc.*, 2005, **127**, 210.

5 D. Massiot, F. Fayon, M. Capron, I. King, S. Le Calve, B. Alonso, J. O. Durand, B. Bujoli, Z. H. Gan and G. Hoatson, *Magn Reson Chem*, 2002, **40**, 70.

6 D. Massiot, S. Drumel, P. Janvier, M. BujoliDoeuff and B. Bujoli, *Chem Mater*, 1997, **9**, 6.